Superconductive and hybrid shielding design: a 3D-modeling study

1st Michela Fracasso
Politecnico di Torino, DISAT
Torino, Italy
michela.fracasso@polito.it

2nd Andrea Napolitano
Politecnico di Torino, DISAT
Torino, Italy
andrea.napolitano@polito.it

3rd Daniele Torsello
Politecnico di Torino, DISAT
Torino, Italy
daniele.torsello@polito.it

4th Laura Gozzelino
Politecnico di Torino, DISAT
Torino, Italy
laura.gozzelino@polito.it

***Abstract*—Superconducting materials are promising for fabrication of high-performance magnetic shields. For this purpose, a computational approach is crucial to guide the shielding devices' design. In this work, we exploit a 3D modeling procedure based on a vector potential formulation to calculate the shielding properties of cup-shaped superconductors (SC) with and without the superimposition of a ferromagnetic (FM) shield. Relying on the past validation of the model, the efficiency of different shielding solutions was investigated in both axial-field (AF) and transverse-field (TF) configurations.**

Keywords—magnetic shielding, 3D numerical modelling, bulk superconductor

I. Introduction

Magnetic shielding is essential for several applications. Its goal is twofold, aiming at the reduction of stray field and electromagnetic noise, and at the achievement of low magnetic field background. Superconductors are key materials for shielding quasi-static magnetic fields [1] - [3]. Recently tested solutions included active [4] and passive layouts [1], [5], [6] . Focusing on the latter, a successful approach to improve shielding ability have combined growth technique able to manufacture properly shaped products with high and homogeneous critical current density, and suitable simulation tools, guiding the whole optimization process [7], [8].

Furthermore, improvements in superconductors (SC) shielding performance have been proved by superimposing a sheet of ferromagnetic (FM) material [9] - [11]. In order to investigate the non-trivial action of adding a FM sheet around the SC [12] and to optimize the shield design under realistic working conditions [13], i.e. for different orientations of applied magnetic field, a 3D modelling is needed.

In this work, we applied the numerical procedure based on the 3D magnetic vector-potential (**A**) formulation described in [14] to predict the shielding properties of a cup-shaped MgB_2 bulks with small height/outer radius aspect ratio, studying the effect of the superimposition of different iron shields in both axial-field (AF) and transverse-field (TF) configurations.

II. Modelling

To model superconductor shielding properties, a numerical procedure based on the magnetic vector potential formalism [14] was applied by a finite element calculation using COMSOL Multiphysics® [15]. As presented in [16], ensuring the collinearity between the current density and the local electric field and considering an isotropic J_c, the following equation can be introduced to relate the current density to the electric field, and, therefore to the time derivative of **A**.

$$\mathbf{J} = \frac{J_c}{|E|}\left(|E_x|tanh\left(\frac{E_x}{E_0}\right)\mathbf{i} + |E_y|tanh\left(\frac{E_y}{E_0}\right)\mathbf{j} + + |E_z|tanh\left(\frac{E_z}{E_0}\right)\mathbf{k}\right) \quad (1)$$

where E_0 is the conventional criterion taken usually as $10^{-4}Vm^{-1}$ [14].

Based on a previous validation of this model to reproduce shielding experiment outputs [17], a J_c dependence on the induction field need also to be taken into account. A previous experiment [18] evidenced that the experimental J_c curves (obtained from magnetic induction cycles measured at different temperatures) were successfully fitted by the exponential relation $J_c(B) = J_{c,0}exp[-(B/B_0)^{\gamma}]$, where $J_{c,0} = 5.02 \times 10^8 A/m^2$, $B_0 = 0.98T$ and $\gamma = 3.78$ were the constant parameters at $T = 30K$. The same parameters were used to model the superconducting shield in all the computations reported in the following.

The magnetic properties of the FM material were defined by the interpolation of the magnetic induction versus applied field curve measured experimentally on a small piece of the soft iron already used to fabricate magnetic shield [11].

The source term for the applied magnetic field, $\mathbf{H_{appl}}$, was considered through the boundary conditions: at a large distance from the shield(s), **B** was set to be equal to $\mu_0\mathbf{H_{appl}}$. The applied field was always assumed increasing monotonically.

III. Numerical results

The model validation presented in [17] allows us to implement the computational procedure in order to explore new hybrid (SC+FM) configurations. Based on previous study outcomes [12], [19], the performances of three different cup-shaped arrangements (Fig.1) were investigated in both AF and TF configurations. The data are then compared with those obtained computing the shielding properties of the SC cup

only, whose dimensions are the same as for the MgB_2 cup studied in [18].

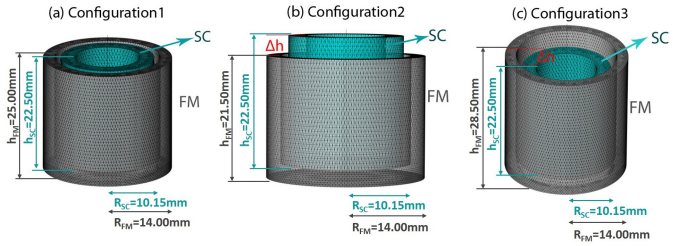

Fig. 1. *Design of cup-shaped hybrid (SC+FM) configurations. SC lateral thickness: 3.15 mm, base thickness: 4.20 mm; FM edge thickness: 2.50 mm, base thickness: 2.50 mm; Δh=3.50 mm.*

For each configuration, the induction field curves along z-axis and y-axis (shown in the insets of Fig.2 and Fig.3, respectively) were computed and the shielding efficiency was estimated using the shielding factor, calculated as the ratio between the applied magnetic field and corresponding component of the local magnetic induction ($SF = \mu_0 H_{app}/B_{z(y)}$). Fig.2 and Fig.3 show the SF behaviors obtained at 5 points along the cup axis in both in AF and TF mode. As one can see, the ferromagnetic sheet addition actually improves the shielding performances.

In particular, for AF configuration and with only SC solution, $SF > 10^2$ and $SF > 10^4$ can be reached up to $\mu_0 H_{app} \approx 1.0$ T in the inner half of the shield and near the closed extremity, respectively (symbols in Fig.2). Adding FM sheet enlarges the high-shielding region up to a field of ≈ 1.2 T, even though at lower fields higher values of SF can not be gained (Fig.2).

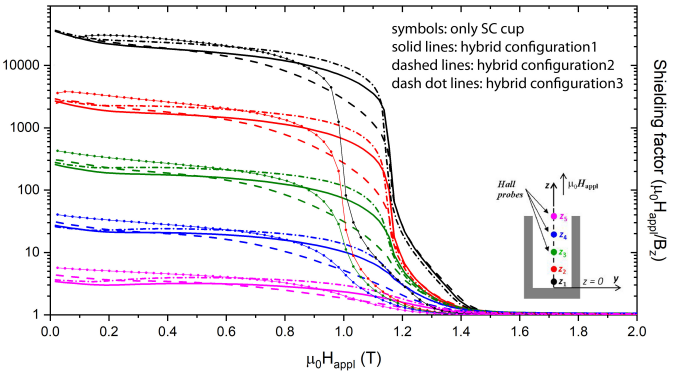

Fig. 2. *Comparison between the SFs of configuration1, 2 and 3 in AF mode considering for the superconductors the same $J_c(B)$ dependence as that measured in [18] at T = 30 K. Assuming (x,y,z) = (0,0,0) the coordinate of the shield center, the plotted curves were calculated at z_1 = 1 mm, z_2 = 5 mm, z_3 = 9.2 mm, z_4 = 13.7 mm and z_5 = 18.3 mm.*

On the other hand, greater enhancements are achieved in TF configuration. The improvements due to the FM addition are twofold. Firstly, likewise in AF geometry, it allows extending the zone where higher SF values are achieved up to above 1.0 T. Secondly, for low values of applied magnetic field, near the closest extremity of the shield, the screening performances improve from a $SF \approx 50$ with only SC (symbols Fig.3) to a $SF \approx 120$ with configuration2 and to a $SF \approx 140$ with configuration3 (Fig.3).

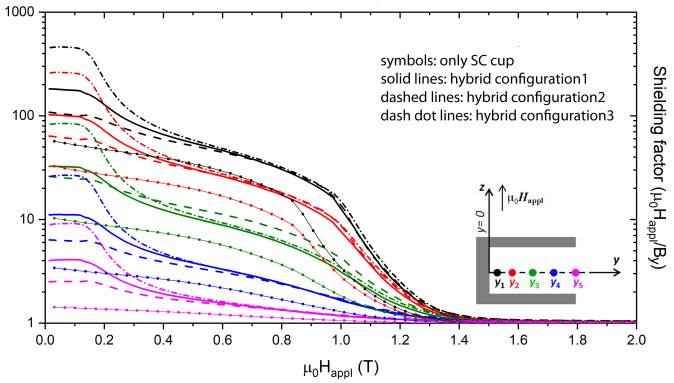

Fig. 3. *Comparison between the SFs of configuration1, 2 and 3 in TF mode considering for the superconductors the same $J_c(B)$ dependence as that measured in [18] at T = 30 K. Assuming (x,y,z) = (0,0,0) the coordinate of the shield center, the plotted curves were calculated at y_1 = 1 mm, y_2 = 4.6 mm, y_3 = 9.2 mm, y_4 = 13.7 mm and y_5 = 18.3 mm.*

These results show how the hybrid system can greatly improve the shielding performances obtained with only superconductor system and evidence how 3D modelling is crucial for achieving a complete information. To this end, the chosen modeling procedure was found to be a valuable tool to drive the design of future magnetic shields with small aspect ratio of height/lateral size and improved shielding performances for various orientations of the applied magnetic field.

ACKNOWLEDGMENT

We wish to thank Fedor Gömöry and Mykola Solovyov for their help in the 3D modelling approach.

REFERENCES

[1] L. Wéra et al., IEEE Trans. Appl. Supercond., 27, 6800305, (2017).
[2] Ł. Tomków et al., J. Appl. Phys., 117,. 043901, (2015).
[3] Y. Terao et al., IEEE Trans. Appl. Supercond., 21, 1584-1587, (2011).
[4] K. S. Haran et al., IEEE Trans. Appl. Supercond., 26, 98-105, (2016).
[5] Barna D et al., IEEE Trans. Appl. Supercond., 29, 4101310, (2019).
[6] J. Durrell et al., Superconductor. Sci. Technol. 31, 103501, (2018).
[7] L. Wéra et al., IEEE Trans. Appl. Supercond, 29, 6801109, (2019).
[8] L. Gozzelino et al., Supercond. Sci. Technol., 32, 034004, (2019).
[9] A. Omura et al., Physica C, 386, 506–511, (2003).
[10] F. Gömöry et al., Science, 335, 1466–1468, (2012).
[11] L. Gozzelino et al., Supercond. Sci. Technol., 25, 115013, (2012).
[12] L. Gozzelino et al., Supercond. Sci. Technol., 29, 034004, (2016).
[13] J. F. Fagnard et al., Supercond. Sci. Technol., 32, 074007, (2019).
[14] M. Solovyov et al., Supercond. Sci. Technol., 32, 115001, (2019).
[15] COMSOL Multiphysics®5.4 software (http://www.comsol.com).
[16] F. Gomory et al., Supercond. Sci. Technol., 22, 034017, (2009).
[17] L. Gozzelino et al., Digest HTS2020(sciencesconf.org:htsmod2020:316157).
[18] L. Gozzelino et al., Supercond. Sci. Technol., 33, 044018, (2020).
[19] G. P. Lousberg et al., IEEE Trans. Appl. Supercond., 20, 33-41, (2010).